



## The radio waves and thermal electrostatic noise spectroscopy (SORBET) experiment on BEPICOLOMBO/MMO/PWI: Scientific objectives and performance

M. Moncuquet <sup>a,\*</sup>, H. Matsumoto <sup>b</sup>, J-L. Bougeret <sup>a</sup>, L.G. Blomberg <sup>c</sup>, K. Issautier <sup>a</sup>,  
Y. Kasaba <sup>d</sup>, H. Kojima <sup>b</sup>, M. Maksimovic <sup>a</sup>, N. Meyer-Vernet <sup>a</sup>, P. Zarka <sup>a</sup>

<sup>a</sup> *Laboratoire d' Etudes Spatiales and Instrumentation en Astrophysique (LESIA), Observatoire de Paris, France*

<sup>b</sup> *Research Institute for Sustainable Humanosphere (RISH), Kyoto University, Japan*

<sup>c</sup> *Royal Institute of Technology (KTH), Alfvén laboratory, Sweden*

<sup>d</sup> *Institute of Space and Astronautical Science (ISAS/JAXA), Kanagawa, Japan*

Received 30 October 2004; received in revised form 26 August 2005; accepted 29 January 2006

### Abstract

SORBET (*Spectroscopie des Ondes Radio and du Bruit Electrostatique Thermique*) is a radio HF spectrometer designed for the radio and Plasma Waves Instrument onboard BepiColombo/Mercury Magnetospheric Orbiter (MMO), which performs remote and in situ measurements of waves (electromagnetic and electrostatic). Technically, SORBET includes a plasma wave spectrometer, with two E-field inputs from the two perpendicular electric antennas and one B-field input from a search coil, in the range 2.5–640 kHz. This frequency band includes the local gyrofrequency and plasma frequency expected on most part of the MMO orbits. SORBET also includes a higher frequency radio receiver for remote sensing in the range 500 kHz–10.2 MHz. Owing to its capabilities, SORBET will be able to address the following scientific objectives:

- High resolution mapping ( $\sim 30$  km) of electron density and temperature in the solar wind and in the Hermean magnetosphere and exosphere, via the technique of Quasi-Thermal Noise (QTN) spectroscopy. These QTN measurements will be determinant for the dynamic modeling of the magnetosphere and will provide a fundamental input for the chemistry of cold ionized species (Na, K, O, ...) in Mercury's environment.
- Detection and study of Hermean radio emissions, including possible cyclotron emissions (up to  $\sim 10$ –20 kHz) from mildly energetic electrons in most highly magnetized (polar?) regions, and possible synchrotron radiation (up to a few MHz?) from more energetic electrons.
- Monitoring of solar radio emissions up to  $\sim 10$  MHz in order to create a solar activity index from the view point of Mercury, allowing to correlate it with the Hermean magnetospheric response.

We especially discuss the capabilities of SORBET for performing the QTN spectroscopy in Mercury's magnetosphere, using the two electric dipole antennas equipping MMO, called MEFISTO and WPT.

© 2006 COSPAR. Published by Elsevier Ltd. All rights reserved.

**Keywords:** Mercury magnetosphere; Thermal noise spectroscopy; Radio and plasma waves; Spacecraft instrumentation; BepiColombo/MMO

\* Corresponding author. Tel.: +33 1 45 07 76 98; fax: +33 1 45 07 28 06.

E-mail address: [michel.moncuquet@obspm.fr](mailto:michel.moncuquet@obspm.fr) (M. Moncuquet).

## 1. Introduction

The SORBET instrument is a spectrometer fitted for the Plasma Waves Instrument (PWI) which is proposed as a part of the scientific payload of the Mercury Magnetospheric Orbiter (MMO). On one hand, SORBET is a thermal noise and plasma wave spectrometer, with two E-field inputs from the WPT and MEFISTO antennas [see also Blomberg et al., 2005a] and one B-field input from the Dual Band Search Coil (DBSC), in the range 2.5–640 kHz, called the TNR band hereinafter. This frequency band will include the local gyrofrequency and plasma frequency on most part of the MMO orbits. On the other hand, SORBET includes a higher frequency radio receiver for remote sensing (measuring only one of the electric antenna signals) in the range 500 kHz–10.2 MHz, called the HFR band hereinafter.

In this paper, we present all the scientific objectives that SORBET should address (Section 2), but we only focus (Section 3) on its specific performances regarding measurement of the electron temperature and density at Mercury, via the technique of Quasi-Thermal Noise (QTN) spectroscopy.

## 2. SORBET's scientific objectives

PWI includes both remote and in situ measurements of wave spectra (electromagnetic and electrostatic), for studying the structure and dynamics (regions, boundaries, acceleration, dissipation processes...) of the Hermean magnetosphere/exo-ionosphere system and its interaction with the solar wind (see e.g., Russell et al., 1988; Slavin, 2004 for reviews). Among these PWI science goals, one may distinguish three specific objectives for the SORBET instrument:

1. Mapping of electron density and temperature in the solar wind and Hermean magnetosphere and exo-ionosphere, via the technique of QTN spectroscopy (including analysis of Bernstein modes and  $f_{uh}$  emissions). We explicit in Section 3 the QTN spectroscopy method and how it will be processed using SORBET and one of the two electric antennas of MMO. These measurements will provide a fundamental input for the chemistry of cold ionized species (Na, K, O, ...) in Mercury's environment and for the dynamic modeling of the magnetosphere (Slavin, 2004). In order to match the simulations of the Hermean magnetosphere, these measurements should have a spatial resolution better than or of the order of the typical proton inertial length at Mercury (Trávníček et al. (2003)), that is from  $\sim 25$  km (at Mercury perihelion  $\sim 0.31$  AU) to 40 km (at Mercury aphelion  $\sim 0.47$  AU). On Fig. 1, we have shown by white or grey area the electron density/temperature ranges that SORBET will be able to measure (the QTN levels and validity domains of the method are explained further in Section 3.2).

Concerning the plasma parameters expected on MMO orbits, the four hatched areas (red and green) plotted on this figure represent typical electron parameters in the solar wind and in the interaction region between the solar wind and the Hermean magnetosphere. The pale pink hatched area corresponds to ranges of  $N_e$  and  $T_e$  usually observed at 1 AU. The two red areas are deduced from the pink one by scaling the previous  $N_e$ – $T_e$  range to Mercury's aphelion (0.47 AU) and perihelion (0.31 AU) according to the gradients observed in the inner heliosphere ( $N_e \propto R^{-2}$  and  $T_e \propto R^{-0.3}$  to  $-0.9$ ). The two green hatched areas are obtained from the red ones by multiplying  $N_e$  by 4 and  $T_e$  by 2 to take into account the compression of the Hermean magnetosheath and are so shown for both the aphelion and perihelion. Corresponding plasma frequencies are expected to be from few tens kHz up to 200–300 kHz. The QTN spectrum should be measured up to at least  $\sim 2 f_{pe}$ , hence  $\geq 600$  kHz. On the other hand, very low densities ( $f_{pe} \sim 1$ –3 kHz) are expected inside the Hermean magnetosphere (simulations show that the density may plummet by factor  $>100$  inward the magnetopause) or in the cusp. For such densities, QTN spectroscopy can be applied if the electron temperature is below  $\sim 10^4$  K (see why in Section 3.1).

2. Detection and study of Hermean radio emissions, including possible cyclotron emissions (up to  $\sim 10$ –20 kHz) from mildly energetic electrons in most highly magnetized (polar?) regions, and possible synchrotron radiation (up to a few MHz?) from more energetic electrons. No stable radiation belts are expected, due to the weakness of Mercury's magnetic field, but intense bursts of energetic particles were measured by Mariner 10 in the magnetotail (Russell et al., 1988). Synchrotron transients could thus be produced from transient radiation belts. Synchrotron emission is a tracer of MeV electrons. It may be remotely detected, provided good instrument sensitivity ( $<15$  nV/Hz $^{1/2}$ ). Short storm-like events with  $\sim 1$  min duration (observed by Mariner 10 – see Russell et al., 1988), as well as Sodium auroras, suggest an auroral activity at Mercury. Associated cyclotron emissions would be produced near fce. From Mariner 10 magnetic measurements,  $B_{max} \sim 400$  nT implies  $f_{ce} \sim 11$  kHz, so that we may expect cyclotron emissions below  $\sim 10$ –20 kHz, in any case trapped with the magnetospheric cavity, as the surrounding solar wind plasma frequency is typically 60–100 kHz [Zarka, 2000]. MMO will perform brief crossings of the region where cyclotron emissions may be detected, and it is important to be able to distinguish without ambiguity between cyclotron emissions and other plasma waves. Their energetic will be compared to that of other planetary radio emissions and with the solar wind magnetic and kinetic energy inputs, to quantify the type and efficiency of the magnetospheric response (reconnection?) to the solar wind. The radio magnetic scaling law [Kaiser and Desch, 1984] predicts an auroral radio power of  $10^{6-7}$  W. It may be much larger if reconnection is very

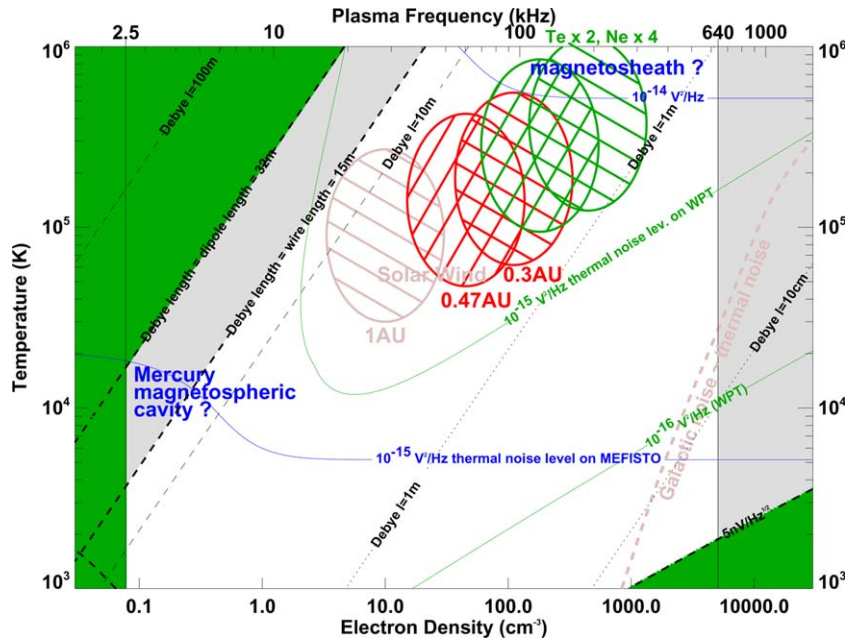


Fig. 1. Diagram of the electron density/temperature accessible (white and gray areas) to SORBET investigations in the TNR band.

effective and/or if energy buffering (storage) takes place prior to sudden dissipation. Distance variations along Mercury’s eccentric orbit ( $e = 0.2$ ) imply variations of a factor 2 of the incident solar wind power (and maybe of auroral radio power). In this frame, the radio emission power density provides a global diagnostic of the magnetospheric activity.

3. Monitoring of solar radio emissions up to  $\sim 10$  MHz (type II and type III radio bursts, indicative of interplanetary transient shocks, CMEs, and energetic particle streams), in order to create a solar activity index from the view point of Mercury, allowing to correlate it with the Hermean magnetospheric response (i.e., “Space

weather” at Mercury). As an illustration, Fig. 2 shows a spectrogram acquired on the WIND spacecraft (located at 1 AU at a Earth Lagrangian point) with our HF receiver, during an intense solar activity.

### 3. A specific requirement: measuring electron density and temperature at Mercury

#### 3.1. Principle of Quasi-Thermal Noise (QTN) measurement

QTN spectroscopy relies upon a fully understood theory and measurements with a simple electric dipole antenna of

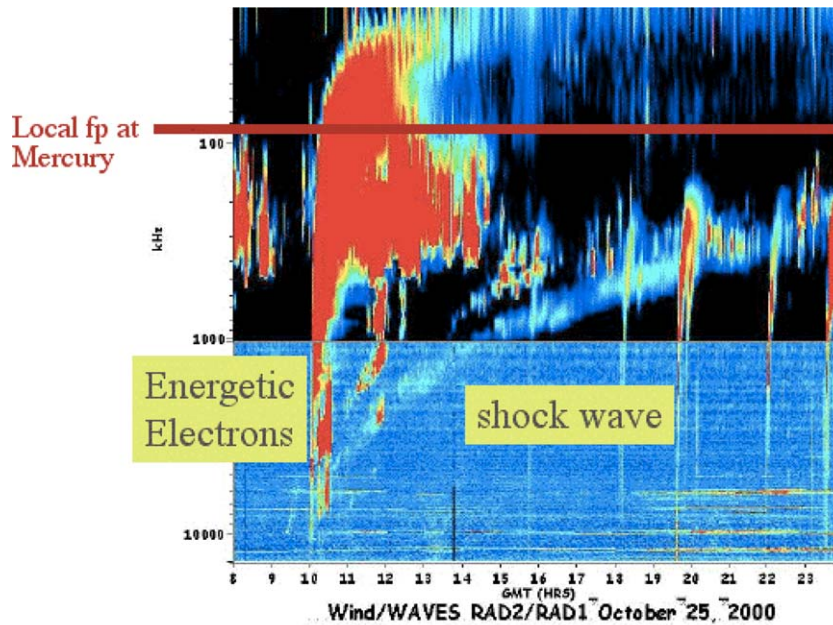


Fig. 2. WIND HF spectrogram. (The frequency range is decreasing from  $\sim 10$  MHz to  $\sim 20$  kHz).

the quasi-thermal fluctuations of the electron population in a plasma [Meyer-Vernet and Perche, 1989]. The quasi-thermal noise is due to the thermal motions of the particles, which produce electrostatic fluctuations. This noise is detected by any sensitive receiver at the ports of an electric antenna immersed in a plasma and can be used to measure in situ the plasma density, temperature, and bulk velocity. The basic reason is that this noise can be formally calculated as a function of both the particle velocity distributions and the antenna geometry. Therefore, conversely, the spectroscopy of this noise reveals the local plasma properties. Theory addresses non-Maxwellian distributions and has been extended to the magnetized case [Moncuquet et al., 1995, 1997] and to the measure of the plasma bulk velocity [Issautier et al., 1999, 2001a]. It provides, without any free parameter fit, measurements with an accuracy of typically  $\sim 1\text{--}2\%$  on  $N_e$ , and  $10\text{--}20\%$  on  $T_e$  down to 300 K (0.03 eV). This is illustrated by the Fig. 3, which shows a power spectrum measured by Ulysses in the solar wind. The measurements are plotted with dots; the best-fitted model of QTN (using a core + halo distribution) is the continuous line. Deduced solar wind parameters are also indicated on this figure. Note that an accurate determination of  $T_e$  and other solar wind parameters requires a sensitive and well-calibrated receiver, while  $N_e$  may be simply deduced from the cutoff frequency of the spectrum. The technique is weakly sensitive to spacecraft potential and photoelectrons perturbations, and it has been (and is still) successfully used on several spacecraft in the solar wind or in planetary magnetospheres/ionospheres (on ISEE3/ICE, Ulysses, Wind, Cassini [see Meyer-Vernet et al., 1998 for a review] and very recently on Cassini at Saturn [Moncuquet et al., 2005]). It has been so frequently used to calibrate  $N_e$  measurements by particle analyzers [Maksimovic et al., 1998; Issautier et al., 2001b].

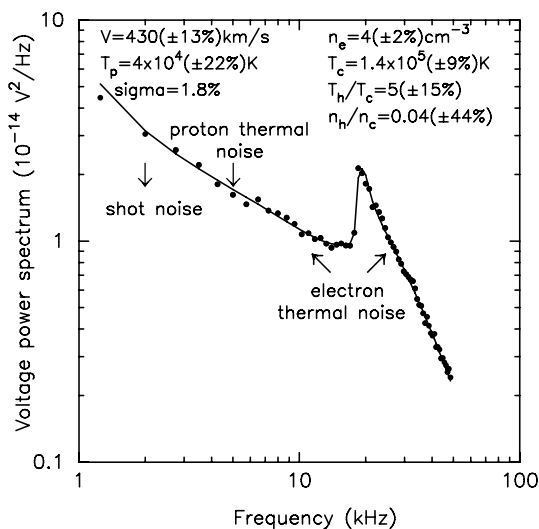


Fig. 3. Quasi-thermal noise spectrum from Ulysses exploited to get solar wind parameters (adapted from Issautier et al., 1999).

### 3.2. SORBET design and capabilities for QTN spectroscopy

On Fig. 1, thermal noise typical levels (green lines for WPT, blue lines for MEFISTO) at frequency immediately below  $f_{pe}$  (thermal plateau) are displayed as a function of the plasma electron density and temperature. These noise levels are computed taking into account both the thermal noise and the shot (or preferably impact) noise contribution, which is of the same order than the thermal noise for sphere probes at  $f \sim f_{pe}$ , while negligible for thin wire antennas. These noise levels are computed for a  $2 \times 15$  m wires + spheres (3 cm radius) antenna and 100 pF of base capacitance for WPT, and a 32 m double sphere (2 cm radius) antenna and 4 pF of base capacitance for MEFISTO (the contribution to thermal noise of the 1–2 m wires on MEFISTO are neglected for a while – see Blomberg et al. (2005b) for a detailed description of the MEFISTO antenna). Lines of constant Debye lengths are also indicated. Then, in the Fig. 1, the white area represents the  $N_e\text{--}T_e$  domain where QTN spectroscopy will provide accurate measurements of the electron plasma parameters for both antennas, and the green areas are the domain where the QTN technique does not apply. For hot and tenuous plasmas, this domain is limited by the fact that the technique requires a dipole length larger than the local Debye length in order to detect adequately the Langmuir wave cutoff and the spectral peak. Therefore, the left gray area shows a domain where the density can be determined but the temperature will be inaccurate, especially on WPT. For dense and cold plasmas, the domain is limited by the preamplifiers noise level (dashed line edging the lower right green zone for a  $5 \text{ nV/Hz}^{1/2}$  noise level on WPT preamps). Finally, the domain is also limited by the frequency range of TNR, but the upper limitation of 640 kHz could be overextended in case of an unlikely high density ( $>6000 \text{ cm}^{-3}$ ) by using the HFR. We show on Fig. 4 two sets of synthesized power spectra for the WPT (right) and MEFISTO (left) antennas, computed with the same antenna inputs than for plotting Fig. 1.

The spectra plotted on Fig. 4 have been computed for four temperatures (with different colors indicated by the chart in the top right corner) and to three plasma frequencies (3, 30, and 200 kHz), easy to distinguish because each spectrum peaks very close to its plasma frequency, except when the corresponding Debye length is larger than the effective antenna length (in which case the spectrum is plotted with a dotted line and is not exploitable for QTN spectroscopy). In order to deal with a realistic plasma, we have also assumed that the velocity distribution is the sum of two Maxwellian distributions (core + halo). For the WPT antenna, the QTN has a thermal plateau immediately below the plasma frequency (and so below the peak), when the impact noise begins to increase at lower frequencies. For MEFISTO, the impact noise contributes to the QTN as  $(f_p/f)^2$  times TN, and is thus dominant below the plasma frequency, so there is no thermal plateau. The noise level is about 5 times larger than on WPT (the dashed horizontal

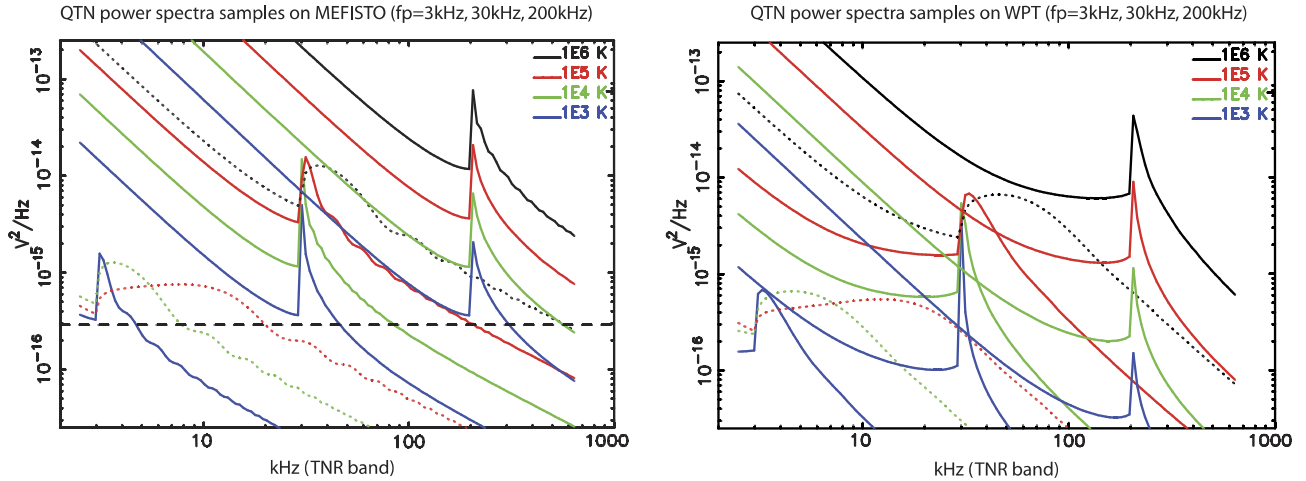


Fig. 4. Some synthesized samples of thermal noise spectral densities collected on WPT (right) and MEFISTO (left).

line on the left panel indicates a preamplifier noise for MEFISTO at  $17 \text{ nV/Hz}^{1/2}$ ). On both antennas, the dynamic range of the QTN is about 40 dB in the whole TNR band and may be  $\sim 10$  dB from the plateau to the peak in a narrow band around the plasma frequency, so that SORBET/TNR must have a wide dynamic range with a very good spectral resolution. On the other hand, the sensors are assumed to have also a wide input dynamic range, low noise preamps (compared to the QTN) and low base capacitance (compared to antenna capacitance). In summary, for both antennas, the Fig. 4 shows that the spectra models are well discriminated by the electron temperature and density variations (and other parameters linked to the hot population not shown here). Stated otherwise, the spectral shapes and levels depend strongly on the plasma thermodynamic parameters; thus the fitting of these models to the measurements will provide accurate values of these parameters.

#### 4. Final remarks and conclusion

Let us first remark that the QTN (including the impact noise) is ubiquitous and may be dominant around the plasma frequency. The QTN will limit the sensitivity threshold of any electric sensor embedded in a plasma, either it is exploited or not for determining plasma parameters. To illustrate this point, we show in Fig. 5 an example of Ulysses spectrum acquired in the solar wind, and where the good knowledge of the QTN collected by the Ulysses electric antenna has allowed us to detect a weak radio emission (in this case a solar type II). This emission level is well above the sensitivity threshold of the Ulysses receiver, but barely emerges from the QTN of the ambient solar wind. In the same way, the detection or absence of detection of the cyclotron emissions expected at Mercury at  $\sim 10\text{--}20$  kHz will depend of the good knowledge of the QTN collected by WPT or MEFISTO.

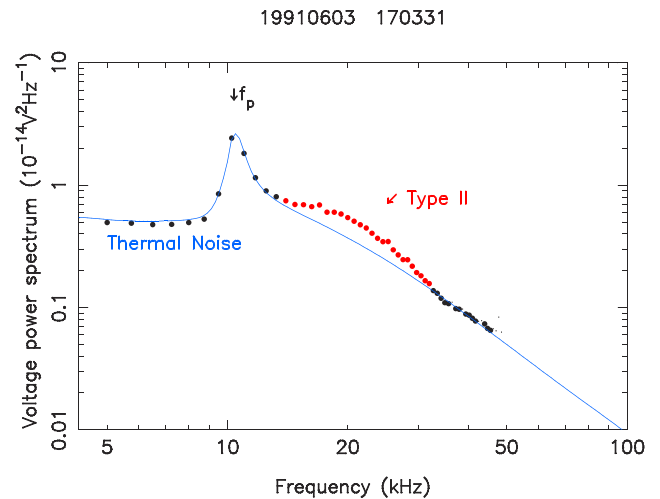


Fig. 5. QTN is ubiquitous and must be subtracted in order to study weak radio emissions, which barely emerges beyond the plasma frequency (from Meyer-Vernet et al. (2000)).

Finally, in order to perform the QTN passive measurement on a pioneering mission as is MMO (such radio measurements will be made at Mercury for the very first time) it is crucial that the corresponding part of the SORBET measurements can be obtained continuously along the MMO orbits. In other words, the measurements in the TNR band need to be recorded, on one of the electric antenna at least, without interruption, that is without triggering nor switching at points predicted from models of the Mercury magnetosphere structure, which is actually unknown. This is of course the very good reason to go and see there with BepiColombo/MMO.

#### References

- Blomberg, L.G., Cumnock, J.A., Kasaba Y., Matsumoto, H., Kojima, H., Omura, Y., Moncuquet, M., Wahlund, J.-E. Electric fields in the

- hermean environment. *Adv. Space Res.*, in press, doi:10.1016/j.asr.2005.02.034, 2005a.
- Blomberg, L.G., Matsumoto, H., Bougeret, J.-L., Kojima, H., Yagitani, S., Cumnock, J.A., et al. MEFISTO – An electric field instrument for BepiColombo/MMO, *Adv. Space Res.*, in press, doi:10.1016/j.asr.2005.05.032, 2005b.
- Issautier, K., Meyer-Vernet, N., Moncuquet, M., Hoang, S., MacComas, D.J. Quasi-thermal noise in a drifting plasma: theory and application to solar wind diagnostic on Ulysses. *J. Geophys. Res.* 104, 6691, 1999.
- Issautier, K., Moncuquet, M., Meyer-Vernet, N., Hoang, S., Manning, R. Quasi-thermal noise diagnostics in space plasmas. *Astrophys. Space Sci.* 277, 309–311, 2001a.
- Issautier, K., Skoug, R.M., Gosling, J.T., Gary, S.P., McComas, D.J. Solar wind plasma parameters on Ulysses: detailed comparison between the URAP and SWOOPS experiments. *J. Geophys. Res.* 106, 15665–15675, 2001b.
- Kaiser, M.L., Desch, M.D. Radio emissions from the planets Earth, Jupiter, and Saturn. *Reviews of Geophysics and Space Physics* 22, 373, 1984.
- Maksimovic, M. et al. Solar wind density intercomparisons on the WIND spacecraft using WAVES and SWE experiments. *Geophys. Res. Lett.* 25, 1265, 1998.
- Meyer-Vernet, N., Perche, C. Tool kit for antennae and thermal noise near the plasma frequency. *J. Geophys. Res.* 94, 2405, 1989.
- Meyer-Vernet, N., Hoang, S., Issautier, K., Maksimovic, M., Manning, R., Moncuquet, M., Stone, R. Measuring plasma parameters with thermal noise spectroscopy, in: Borovsky, E., Pfaff, R. (Eds.) *Geophysical Monograph 103: Measurements Techniques in Space Plasmas*, pp. 205–210, 1998.
- Meyer-Vernet, N., Hoang, S., Issautier, K., Moncuquet, M., Marcos, G. Plasma thermal noise: the long wavelength radio limit, *Geophysical Monograph 119: Radio Astronomy at Long Wavelengths* (ISSN 0065–8448), pp. 67–78, 2000.
- Moncuquet, M., Meyer, N., Hoang, S. Dispersion of electrostatic waves in the Io plasma torus and derived electron temperature. *J. Geophys. Res.* 100, 21697–21708, 1995.
- Moncuquet, M., Meyer, N., Hoang, S., Forsyth, R.J., Canu, P. Detection of Bernstein wave forbidden bands in the Jovian magnetosphere: a new way to measure the electron density. *J. Geophys. Res.* 102, 2373–2379, 1997.
- Moncuquet, M., Lecacheux, A., Meyer-Vernet, N., Cecconi, B., Kurth, W.S. Quasi thermal noise spectroscopy in the inner magnetosphere of Saturn with Cassini/RPWS: electron temperatures and density. *Geophys. Res. Lett.* 32, L20S02, doi:10.1029/2005GL022508, 2005.
- Russell, C.T., Baker, D.N., Slavin, J.A. *The Magnetosphere of Mercury, in Mercury (A89-43751 19-91)*, Tucson, AZ, University of Arizona Press, pp. 514–561, 1988.
- Slavin, J.A. Mercury's Magnetosphere. *Adv. Space Res.* 33 (11), 1859–1874, 2004.
- Trávníček, P., Hellinger, P., Schriver, D. A global three dimensional hybrid simulation of the interaction between a weakly magnetized obstacle and the solar wind, *Proceedings of SW10. AIP* 679, 485–488, 2003.
- Zarka, P. Radio emissions from the Planets and their Moons, *Geophysical Monograph 119: Radio Astronomy at Long Wavelengths*, pp. 167–178, 2000.